DEUTSCHES ELEKTRONEN-SYNCHROTRON DESY

DESY 83-108
October 1983

受入
83-12-83
高工研図書室

# FIRST RESULTS FROM THE CRYSTAL BALL AT DORIS II

by

A. Schwarz

*I. Institut für Experimentalphysik, Universität Hamburg*

ISSN 0418-9833

NOTKESTRASSE 85 · 2 HAMBURG 52

DESY behält sich alle Rechte für den Fall der Schutzrechtserteilung und für die wirtschaftliche Verwertung der in diesem Bericht enthaltenen Informationen vor.

DESY reserves all rights for commercial use of information included in this report, especially in case of apply for or grant of patents.

To be sure that your preprints are promptly included in the
HIGH ENERGY PHYSICS INDEX ,
send them to the following address ( if possible by air mail ) :

DESY
Bibliothek
Notkestrasse 85
2 Hamburg 52
Germany

DESY 83-108
October 1983

ISSN 0418-9833

# First Results from the CRYSTAL BALL AT DORIS II*

presented by

Andreas Schwarz

I. Institut für Experimentalphysik der Univ. Hamburg
Luruper Chaussee 149, D-2000 Hamburg 50

Representing

The Crystal Ball Collaboration[a]

The Crystal Ball has been installed at DORIS II and taking data since the fall of 1982. Data have been obtained at the $\Upsilon(1S)$, $\Upsilon(2S)$ and the continuum region just below the $\Upsilon(2S)$. Preliminary results of the analyses of these data are presented. These results include inclusive photon spectra from the $\Upsilon(1S)$ and $\Upsilon(2S)$ and the transitions $\Upsilon' \to \pi^0\pi^0\Upsilon$ and $\Upsilon' \to \gamma\gamma\Upsilon$.

*Talk given at the International Europhysics Conference on High Energy Physics, Brighton (UK), 20-27 July, 1983.



## (1) Introduction

The Crystal Ball has taken data at DORIS II since August 1982. Its main goal was to study the physics of the $b\bar{b}$-system (b = bottom-quark) focusing on the electromagnetic radiative decays of the $\Upsilon(2S)$. Fig. 1 is a rough sketch of the theoretically expected energy levels of the bound bottonium system below the $\Upsilon(2S)$. The $\Upsilon(2S)$ can decay radiatively via emission of a real photon to the P-wave states $^3P_{2,1,0}$ which subsequently decay hadronically or again via emission of a second photon to the ground state, the $\Upsilon(1S)$. The determination of the masses of the P-states would yield important insight into various aspects of the interquark potential. The center of gravity (c.o.g.) of the 3 states tests mainly the shortrange behaviour of the interquark force. As an example a pure coulombic potential would give $M(\Upsilon(2S))-M(\text{c.o.g.}) \simeq 0$. The total splitting $\Delta M = M(^3P_2)-M(^3P_0)$ as well as the individual fine structure splittings, expressed in the form

$$r = \frac{M(^3P_2) - M(^3P_1)}{M(^3P_1) - M(^3P_0)}$$

on the other hand gives information about the spin dependent part of the potential. The $\Upsilon$ system should be a very good testing ground especially for the spin dependent part of the potential because it is not as relativistic as the $J/\psi$ system which made the ansatz of a potential problematic, but it is still relativistic enough that one can hope to be able to measure some relativistic effects, namely the P-wave splitting. The expectation, however, is that the measurements will be much harder on the $\Upsilon(2S)$ than on the $\psi'$ due to several factors:

- The signal to noise ratio is about 1/10 to 1/15 of that at the $\psi'$.
- Due to the higher multiplicities compared to the $\psi'$ center-of-mass energies, the photon detection efficiencies will be lower because of overlap problems.
- We have a much larger contamination from nonresonant continuum events. (The ratio of the number of resonance events to the number of continuum events per unit of integrated luminosity is roughly 1:1.)

(2) The Crystal Ball at DORIS II

The Crystal Ball detector (Fig. 2) consists mainly of a spherical segmented shell of NaI(Tl) shower counters which cover 93% of $4\pi$ solid angle. This coverage is increased to 98% of $4\pi$ by NaI(Tl) endcaps. The direction of charged particles is measured in 3 double layers of proportional tube chambers with charge division readout. The Crystal Ball in its configuration at SPEAR has been described in detail elsewhere (1). At DORIS the endcap design as well as the luminosity monitor system were modified to allow space for the mini beta quadrupoles.

The thickness of the NaI(Tl) shell corresponds to 16 radiation lengths and to one nuclear absorption length for high energy pions. The distribution of energy deposited by charged hadrons peaks at around 200 MeV due to non interacting minimum ionizing charged particles and has a long tail caused by nuclear interactions. Neutral electromagnetically decaying hadrons deposit all their energy in the detector. The energy resolution of the detector for photons or electrons is measured to be

$$\sigma_E/E = (0.024-0.028)/E^{1/4} \quad (E \text{ in GeV})$$

The data accumulated by the detector to the beginning of July are listed in Table I. Fig. 3 shows a scan across the two resonances $\Upsilon(1S)$ and $\Upsilon(2S)$. The $\Upsilon(2S)$ resonance contribution over the continuum background is only $\Delta R_{vis} \approx 3.3$ (where $R_{vis}$ is the visible hadronic cross section normalized to the $\mu$-pair cross-section $\sigma_{\mu\mu}$).

Fig. 4a shows a distribution of the invariant gamma-gamma mass which one gets forming in each hadronic event all possible different combinations of two photons. One clearly sees a peak at the mass of the $\pi^0$. A fit to the region around the $\pi^0$-mass with a gaussian signal and a polynomial background yields for the mass a value of $(133\pm0.3)$ MeV/$c^2$.

If one rejects all photon pairs which form a $\pi^0$ (Fig. 4b), one can see a signal in the region of the $\eta$ (548). A fit to this signal gives M = $(535\pm3)$ MeV/$c^2$. One notices that these masses are low



by about 2-3% compared to the world average (2) indicating that we have a systematic uncertainty in our energy scale. This was also observed during SPEAR running.

Another check to see whether the detector works properly is the study of exclusive decay modes of the $\Upsilon(2S)$. An example of such a decay is

$$\Upsilon(2S) \to \pi^0\pi^0\Upsilon(1S) \to \gamma\gamma\gamma\gamma\ell^+\ell^-$$

where the $\Upsilon(1S)$ may be detected by its decay into leptons. Fig. 5a shows the two dimensional distribution of $M_{\gamma_1\gamma_2}$ vs. $M_{\gamma_3\gamma_4}$ where $M_{\gamma_1\gamma_2}$ is the invariant gamma-gamma mass formed out of two of the four photons in the event and $M_{\gamma_3\gamma_4}$ is the corresponding quantity for the remaining two photons. (Note that there are 3 such combinations for each event in Fig. 5a). A clear signal is observed in a region where both gamma-gamma combinations of the event give the $\pi^0$-mass. Performing a cut in a 2.5 sigma window around the $\pi^0$-mass as indicated in Fig. 5a, we plot the mass difference

$$\Delta M = M(\Upsilon(2S)) - M_{recoil}.$$

$M_{recoil}$ is the mass of the system which recoils against the 4 photons and thus should lie in the region of the $\Upsilon(1S)$-mass. $\Delta M$ should therefore peak at the mass difference of $M(\Upsilon(2S))-M(\Upsilon(1S)) \approx 560$ MeV/$c^2$ (3).

A clear peak with mean $(542\pm3)$ MeV and width $(14\pm2)$ MeV is observed. The width is consistent with the energy and angular resolution of the detector. The mean value is about 3 % low again indicating our systematic uncertainty in the energy scale.

Fig. 6 shows the distribution of the invariant mass of the $\pi^0\pi^\pm$-system after a cut in the quantity $\Delta M$ as indicated in Fig. 5b. This mass distribution is peaked towards high values; this fact has also been observed in the charged pion mode, $\Upsilon' \to \pi^+\pi^-\Upsilon$ (4).

(3) The Inclusive Photon Spectrum

The search for radiative decays of the T(2S) to the $^3P_{2,1,0}$ states can either be made by measuring the inclusive photon spectrum of the process

$$T(2S) \rightarrow \gamma + \text{hadrons}$$

or by determining the exclusive photon spectrum in the process

$$T(2S) \rightarrow \gamma {}^3P_{2,1,0} \; ; \; {}^3P_{2,1,0} \rightarrow \gamma T(1S); \; T(1S) \rightarrow e^+e^- \text{ or } \mu^+\mu^-$$

Here we first want to inspect the inclusive photon spectrum.

The photon selection criteria used in this analysis were:

- A photon must lie well within the ball which means $|\cos\theta_\gamma| < 0.75$ where $\theta_\gamma$ is the angle of the photon direction with respect to the beam. This cut ensures that the track lies within the solid angle covered by all 3 tracking chambers.
- It has to be 'neutral' which means that it has no track-correlated hit in the tracking chambers.
- Its lateral energy deposition must be consistent with that of a single electromagnetic shower.

In addition, all photon pairs are removed which form a $\pi^0$. The resulting photon detection efficiency ranges from about 22% at 100 MeV photon energy to about 38% at 500 MeV. The systematic uncertainty in this efficiency is estimated to be 20%. The inclusive photon spectra for our entire T(2S) and T(1S) data after imposing the above cuts are displayed in Fig. 7. A clear structure is seen in the T(2S)-spectrum at 100-150 MeV and around 430 MeV whereas the T(1S)-data do not show a significant signal. Fits to the 100-180 MeV and 300-600 MeV regions of the T(1S)-spectrum give no signal which has a significance of more than two standard deviations.

A fit to the low energy region of the $\gamma$-spectrum with a quadratic background and two gaussians with their widths determined by our energy resolution of $\sigma_E/E = 0.024/E^{1/4}$ gives a $\chi^2$ per degree of freedom of 7.4/20 (Fig. 8a).



The energies of the two observed lines, the significance (number of standard deviations (s.d.) away from zero) and the resulting calculated branching ratios (BR) of the process T(2S) $\rightarrow \gamma$ + hadrons, are

| $E_\gamma$ [MeV] | significance (s.d.) | BR (%) |
|---|---|---|
| 108.3±0.9 | 4.8 | (6.3±1.3±1.4) |
| 127.5±1.2 | 5.0 | (6.0±1.3±1.4) |

Note that the calculation of branching ratios assumes an isotropic distribution for the photon. The systematic error on the photon energies is ±3%.

The above numbers compare well with the values measured by the CUSB collaboration recently (5). In addition to these two lines, they fitted a third line to their data which gave $E_\gamma$ = (149.4±0.7±5.0) MeV. We have tried adding a third gaussian folded with a Breit-Wigner lineshape to the two gaussians over the quadratic background. We tried two assumptions:

(α) the intrinsic width of the Breit-Wigner is negligible compared to the energy resolution and so the observed line width is fully determined by the resolution of the detector and
(β) the third line corresponds to a broad resonance with an intrinsic Breit-Wigner width of 10 MeV.

The mean energy of the third line was then systematically varied over a region from 145 MeV to 155 MeV and at each point, we calculated our upper limit for observing a third line. The result of this procedure is displayed in Fig. 9 which shows the Crystal Ball upper limit on the branching ratio to a hypothetical third line as a function of the mean of the photon energy compared to the value of CUSB.

We can therefore give the following upper limits for the branching ratio at the 90% confidence level:

| $E_\gamma$ [MeV] | significance (s.d.) | BR (%) |
|---|---|---|
| 144-155 | <1 | <4.5 for a broad state |
| | | <3.0 for a narrow state |

The calculation of these upper limits assumes a $(1+\cos^2\theta)$-distribution for the photon as expected for the decay $\Upsilon(2S) \to \gamma\,^3P_J$. For an isotropic decay it would be about 10% lower. The above quoted results for the other two lines were not affected by this procedure.

A fit to the region around 430 MeV with one gaussian plus a quadratic background shows that the observed width is wider than expected from our energy resolution. Using two gaussians and fitting this region together with the observed lines at 108 MeV and 128 MeV under the assumption that they all belong to the cascade $\Upsilon(2S) \to \gamma\,^3P_J$, $^3P_J \to \gamma\Upsilon(1S)$ (Fig. 8b) gives a measure of the mass difference $\Delta m = m(\Upsilon(2S)) - m(\Upsilon(1S))$ of

$$\Delta m = (555.3 \pm 5.9)\ \text{MeV}$$

which is a very good indication for the validity of the cascade hypothesis. The observed line is consistent with either or both primary lines cascading to the $\Upsilon(1S)$. The resulting branching ratio for the process $\Upsilon(2S) \to \gamma$ + hadrons is

| $E_\gamma$ [MeV] | significance (s.d.) | BR (%) |
|---|---|---|
| 426 | 3.9 | $(3.6 \pm 0.9 \pm 0.8)$ |

and may be interpreted as the sum of the individual product branching ratios

$$BR(\Upsilon(2S) \to \gamma_{108} + {}^3P_J) \cdot BR({}^3P_J \to \gamma_{437} + \Upsilon(1S)) +$$
$$BR(\Upsilon(2S) \to \gamma_{128} + {}^3P_{J'}) \cdot BR({}^3P_{J'} \to \gamma_{417} + \Upsilon(1S)).$$

(4) Exclusive Cascade Analysis

As a consistency check for the inclusive event analysis we looked for the exclusive channel

$$\Upsilon(2S) \to \gamma\,^3P_J \hookrightarrow \gamma\Upsilon(1S) \hookrightarrow e^+e^- \text{ or } \mu^+\mu^-\,.$$



The event selection required

- 4 particles in the main ball (not in the tunnel region) which requires for each track $|\cos\theta| < 0.90$ where $\theta$ is the polar angle with respect to the positron direction.
- 2 of the 4 particles must be back to back leptons with $\cos\alpha_{ij} < -0.85$. The electron candidates must have a track energy in the region $3500 < E < 6200$ MeV. Muon candidate tracks should have an energy deposition consistent with that of a minimum ionizing particle, i.e. between 150 and 300 MeV. This energy should be deposited in a very small number of adjacent crystals (typically 1-3 crystals).
- The remaining two particles in the event (the photon candidates) must have an energy exceeding 50 MeV each and should not lie too near other tracks ($\cos\alpha_{ij} < 0.9$).

Events surviving these cuts were then subjected to a kinematic fit to the hypothesis $\Upsilon(2S) \to \gamma\gamma\ell^+\ell^-$ ($\ell^\pm$ = lepton) which checks whether the event is kinematically fully determined. This is a four constraint (4-C-) fit in the case $\Upsilon(2S) \to \gamma\gamma e^+e^-$ because all four momenta of the final state are measured and a 2-C-fit in the case $\Upsilon(2S) \to \gamma\gamma\mu^+\mu^-$ because only the directions are determined for the muons.

Events which had a confidence level of less than 10% in this fit were rejected.

Fig. 10a shows the energy of the lower energetic photon plotted against the quantity

$$\Delta M = M(\Upsilon(2S)) - M_{recoil}$$

where $M_{recoil}$ is the missing mass recoiling against the two photons in the event. A clear clustering is seen in a band around approximately the mass difference of the $\Upsilon(2S)$ and the $\Upsilon(1S)$ (taking into account our systematic energy scale-uncertainty of the order of 2-3%). The projection of this distribution onto the $\Delta M$-axis is displayed in Fig. 10b. To survive our final selection, the events must lie inside a ±3 standard deviation band around the mass difference as measured by the channel $\Upsilon(2S) \to \pi^0\pi^0 ee$ (see above) (cut region: 545±45 MeV).

In Fig. 11a,b, a projection of all the modules comprising the ball proper is displayed showing events of the type $\Upsilon(2S) \to \gamma\gamma e^+e^-$ and $\Upsilon(2S) \to \gamma\gamma\mu^+\mu^-$ which survived all the above mentioned cuts. Each triangle corresponds to one NaI(Tl) module with the measured energy appearing in MeV.

We found 46 events in our data sample (20 $\gamma\gamma e^+e^-$, 26 $\gamma\gamma\mu^+\mu^-$) satisfying our selection criteria. The energy spectrum of the lower energy photons in the region of interest is shown in Fig. 12. The energies are uncorrected for systematic calibration errors. Fitting this spectrum with two gaussians with widths fixed according to our energy resolution and a flat background (histogram in Fig. 12) yields

$$E_{\gamma_1} = (102\pm2\pm4)\ \text{MeV}$$
$$E_{\gamma_2} = (127\pm2\pm4)\ \text{MeV}$$

with a confidence level of 70%. This is consistent with the result of the inclusive photon analysis in position as well as in width.

(5) Conclusion

Using the Crystal Ball at DORIS II, we have observed two photon lines of the transition $\Upsilon(2S) \to \gamma^3P_J$: one at $E_\gamma = (108.3\pm0.9)$ MeV with a branching ratio of BR = $(6.3\pm1.3\pm1.4)$% and the other one at $E_\gamma = (127.5\pm1.2)$ MeV with a branching ratio of BR = $(6.0\pm1.3\pm1.4)$%. These results are consistent with the values measured by the CUSB collaboration. We observed a third line at $\langle E_\gamma \rangle \simeq 426$ MeV which is in position and width consistent with being the second line of the cascade $\Upsilon(2S) \to \gamma^3P_J$, $^3P_J \to \gamma\Upsilon(1S)$. The product branching ratio for these processes is BR = $(3.6\pm0.9\pm0.8)$%.

With our present statistics,we do not observe a third line in the region 145 MeV < $E_\gamma$ < 155 MeV. We therefore set an upper limit on the branching ratio for a third line in this region of

BR < 4.5% under the assumption of a broad state ($\Gamma$ = 10 MeV) (90% confidence level)

BR < 3.0% under the assumption of a narrow state ($\Gamma$ = 0 MeV) (90% confidence level).



Using the results of the inclusive photon spectrum, the mass splitting between the two observed states is

$$\Delta M(^3P_J - ^3P_{J'}) = (19.4\pm2.0)\ \text{MeV}/c^2.$$

Without a spin/parity measurement, we cannot assign quantum numbers to the observed states.

References

(a) The Crystal Ball Collaboration:
C. Edwards, C. Peck, F. Porter, P. Ratoff (California Institute of Technology, Pasadena, USA); I. Brock, A. Engler, R. Kraemer, D. Marlow, F. Messing, D. Prindle, B. Renger, C. Rippich (Carnegie-Mellon University, Pittsburgh, USA); Z. Jakubowski, B. Niczyporuk, G. Nowak, T. Skwarnicki (Cracow Institute of Nuclear Physics, Cracow, Poland); J.K. Bienlein, S. Cooper, B. Gomez, T. Kloiber, W. Koch, M. Schmitz, H.-J. Trost, P. Zschorsch (Deutsches Elektronen-Synchrotron DESY, Hamburg, Germany); D. Antreasyan, J. Irion, K. Strauch, D. Williams (Harvard University, Cambridge, USA); D. Besset, R. Cabenda, M. Cavalli-Sforza, R. Cowan, D. Coyne, C. Newman-Holmes (Princeton University, Princeton, USA); E. Bloom, R. Chestnut, R. Clare, J. Gaiser, G. Godfrey, S. Leffler, W. Lockman, S. Lowe, K. Wacker (Stanford Linear Accelerator Center, Stanford University, USA); D. Gelphman, R. Hofstadter, I. Kirkbride, R. Lee, A. Litke, T. Matsui, B. Pollock, J. Tompkins (Stanford University, Department of Physics and HEPL, Stanford, USA); G. Folger, B. Lurz, U. Volland, H. Wegener (Universität Erlangen-Nürnberg, Erlangen, Germany); A. Cartacci, G. Conforto, D. de Judicibus, B. Monteleoni, P.G. Pelfer (INFN and University of Firenze, Italy); A. Fridman, F.H. Heimlich, R. Lekebusch, P. Lezoch, W. Maschmann, R. Nernst, A. Schwarz, D. Sievers, U. Strohbusch (Universität Hamburg, I. Institut für Experimentalphysik, Hamburg, Germany); A. König, J. Schotanus, R.T. Van de Walle, W. Walk (University of Nijmegen, The Netherlands); S. Keh, H. Kilian, K. Königsmann, M. Scheer, P. Schmitt (Universität Würzburg, Germany); D. Aschman (University of Cape Town, South Africa).

(1) M. Oreglia, Ph. d. Thesis, Stanford University, SLAC-236 (1980)
M. Oreglia et al., Phys. Rev. D25(1982)2259
J. Gaiser, Ph. d. Thesis, Stanford University, SLAC-255 (1982)

(2) Particle Data Group, Review of Particle Properties, Phys. Lett. 111B(1982)

(3) D.P. Barber et al., DESY-Preprint, DESY 83-067, July 1983

(4) B. Niczyporuk et al., Phys. Lett. 100B(1981)95
J.J. Muller et al., Phys. Rev. Lett. 46(1981)1181

(5) C. Klopfenstein et al., Phys. Rev. Lett. 51(1983)160



Table I: The accumulated Crystal Ball data as of July 1983.

| | Integrated luminosity [$pb^{-1}$] | Observed hadronic decays ($\cdot 10^3$) | Resonance decays ($\cdot 10^3$) |
|---|---|---|---|
| $\Upsilon(1S)$ | 7.8 | 67 | 53±6 |
| $\Upsilon(2S)$ | 24.5 | 121 | 66±7 |

Figure Captions:

Fig. 1: The theoretically expected energy levels of the bound bottonium system below the $\Upsilon(2S)$.

Fig. 2: The Crystal Ball Detector at DORIS II.

Fig. 3: The ratio of the visible hadronic cross section and the $\mu$-pair cross section as a function of the center of mass energy in the region of the $\Upsilon(1S)$ and the $\Upsilon(2S)$.

Fig. 4a: The distribution of the invariant gamma-gamma mass.

Fig. 4b: Same as 4a, but all photon pairs which form a $\pi^0$ have been removed.

Fig. 5a: $M_{\gamma_1\gamma_2}$ vs. $M_{\gamma_3\gamma_4}$ for events of the type $\Upsilon(2S) \to \gamma\gamma\gamma\gamma e^+e^-$. $M_{\gamma_i\gamma_j}$ is the invariant mass formed out of the photons i and j.

Fig. 5b: The mass difference $\Delta M = M(\Upsilon(2S)) - M_{recoil}$ for events of the type $\Upsilon(2S) \to \gamma\gamma\gamma\gamma\ell^+\ell^-$. $M_{recoil}$ is the mass of the system which recoils against the 4 photons in the event. The value of the mass difference and the width of the distribution is consistent with our energy resolution.

Fig. 6: The invariant mass of the $\pi^0\pi^0$-system of events of the type $\Upsilon(2S) \to \pi^0\pi^0\Upsilon(1S)$.

Fig. 7: The inclusive photon spectra for our $\Upsilon(2S)$ and $\Upsilon(1S)$ data.

Fig. 8a: A fit to the low energy region of the inclusive photon spectrum of the $\Upsilon(2S)$ using 2 gaussians over a quadratic background.

Fig. 8b: A fit to the region around 430 MeV of the inclusive photon spectrum of the $\Upsilon(2S)$ using 1 gaussian over a quadratic background.

Fig. 9: The Crystal Ball upper limit on the branching ratio to a hypothetical third line as a function of the mean photon energy. Also shown is the CUSB value at 149 MeV.



Figure Captions:

Fig. 10a: The energy distribution of the low energetic photons for events of the type $\Upsilon(2S) \to \gamma\gamma\ell^+\ell^-$ ($\ell^\pm$: leptons) plotted against the mass difference $\Delta M = M(\Upsilon(2S)) - M_{recoil}$. $M_{recoil}$ is the missing mass recoiling against the two photons in the event. The mean and the width of the distribution is consistent with the ones in Fig. 5b.

Fig. 10b: The projection of Fig. 10a onto the $\Delta M$-axis.

Fig. 11a: A projection of all the modules comprising the ball proper showing an event of the type $\Upsilon(2S) \to \gamma\gamma e^+e^-$.

Fig. 11b: As Fig. 11a, showing an event of the type $\Upsilon(2S) \to \gamma\gamma\mu^+\mu^-$.

Fig. 12: The energy spectrum of the low energetic photons in the events of the type $\Upsilon(2S) \to \gamma\gamma\ell^+\ell^-$ ($\ell^\pm$: leptons).

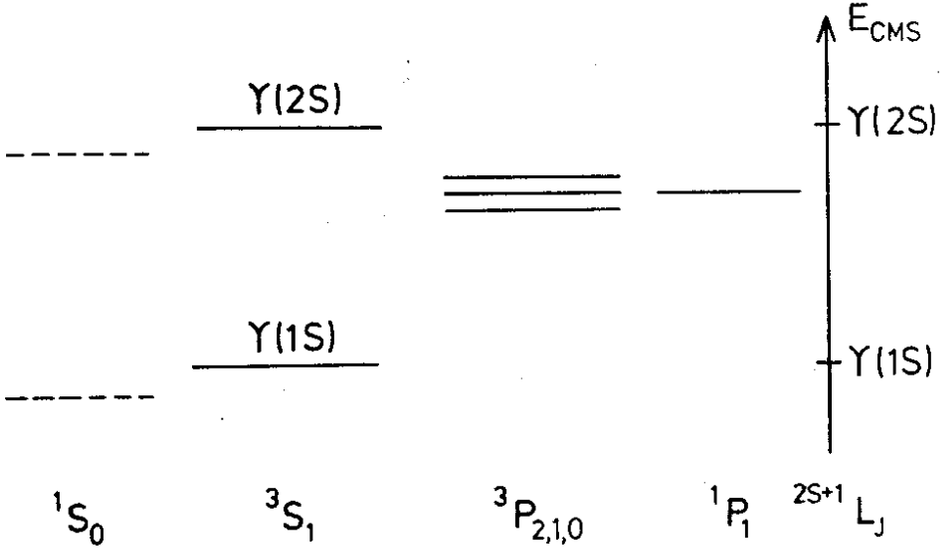


Fig.1

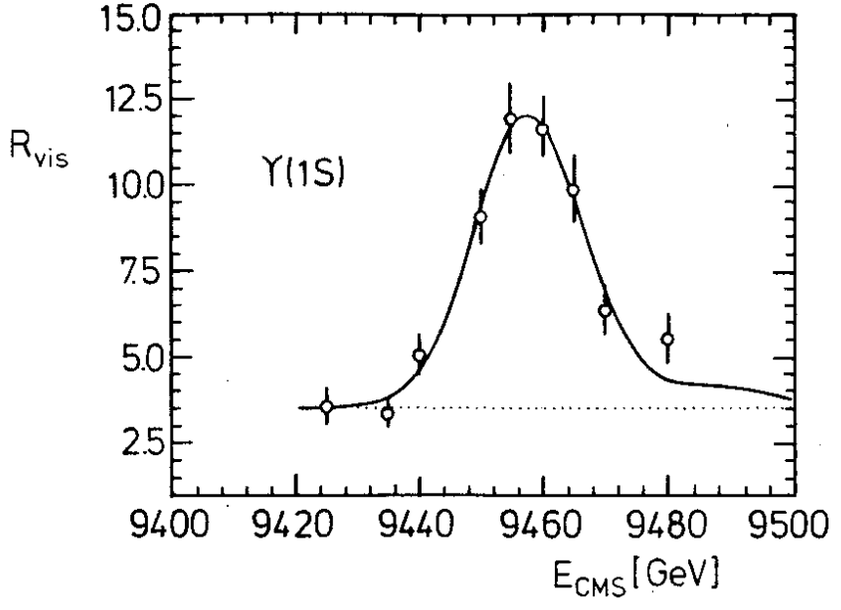


Fig.3

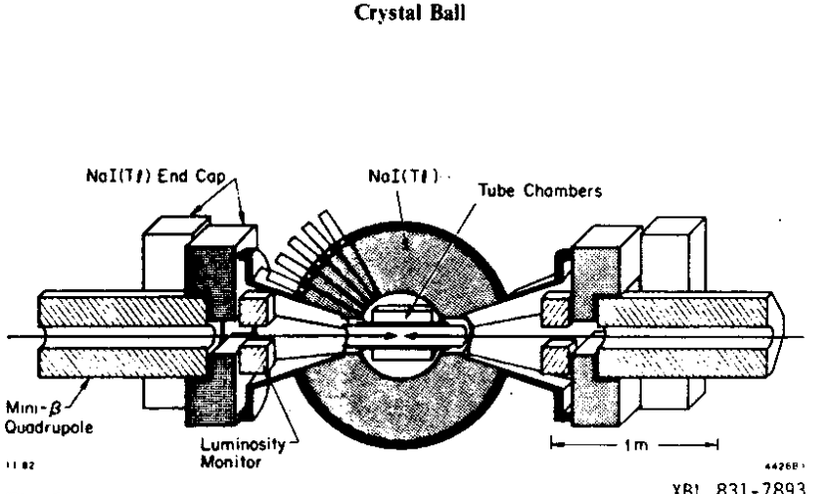


Fig.2

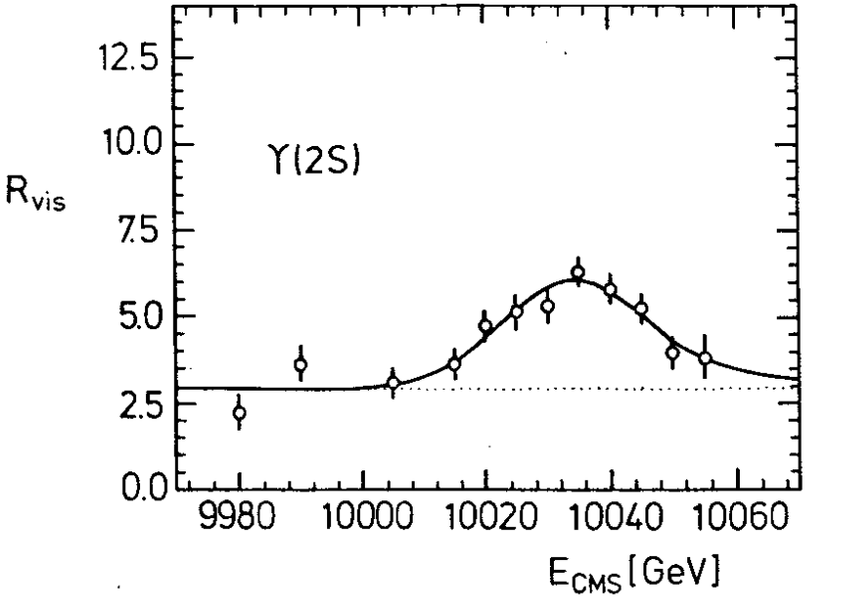

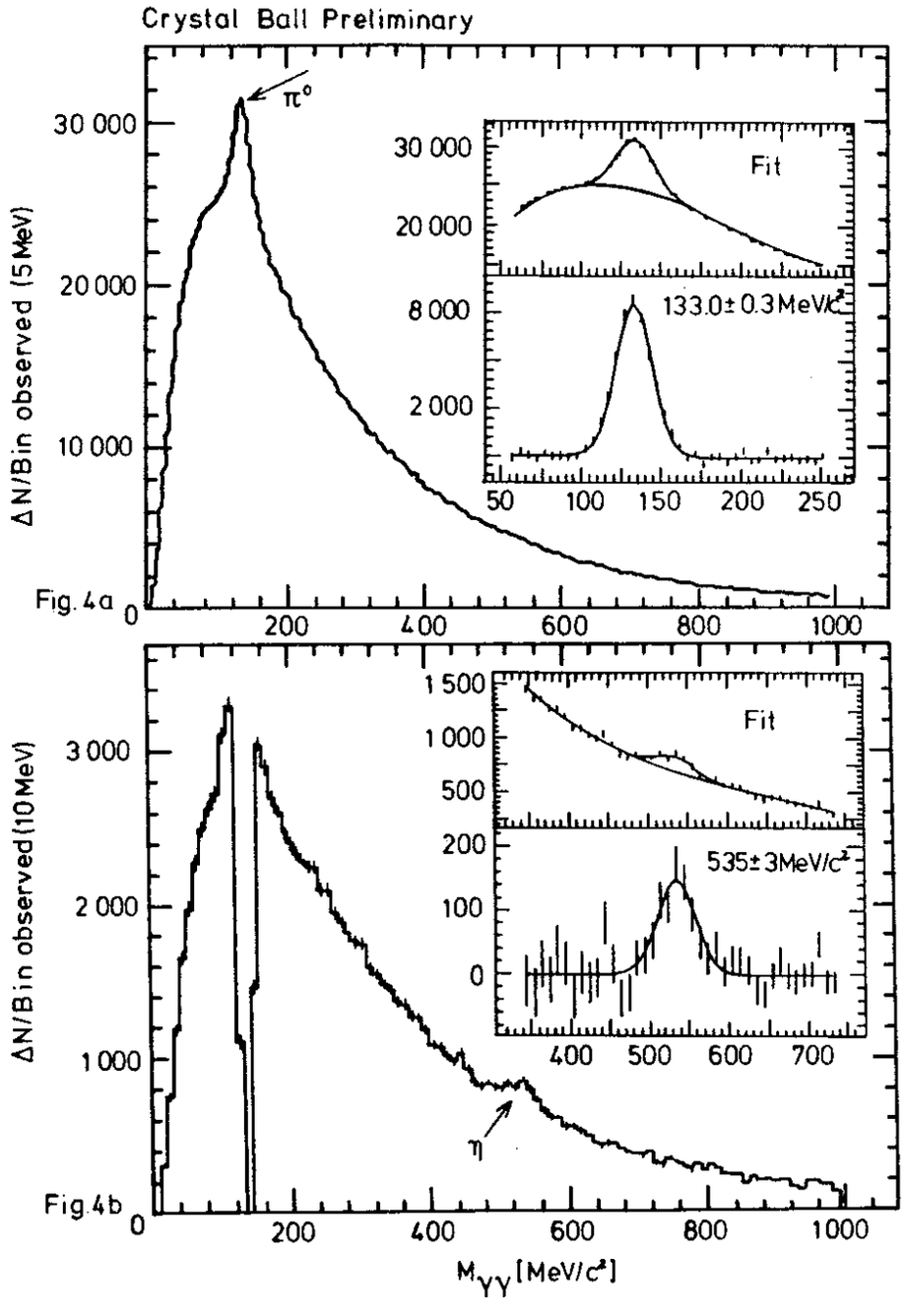
Crystal Ball Preliminary
π°
ΔN/Bin observed (5 MeV)
30 000
20 000
10 000
0
Fit
133.0± 0.3 MeV/c²
8 000
2 000
50 100 150 200 250
200 400 600 800 1000
Fig. 4a
ΔN/Bin observed (10 MeV)
3 000
2 000
1 000
0
1 500
1 000
500
200
100
Fit
535± 3 MeV/c²
400 500 600 700
η
Fig. 4b
200 400 600 800 1000
M_γγ [MeV/c²]

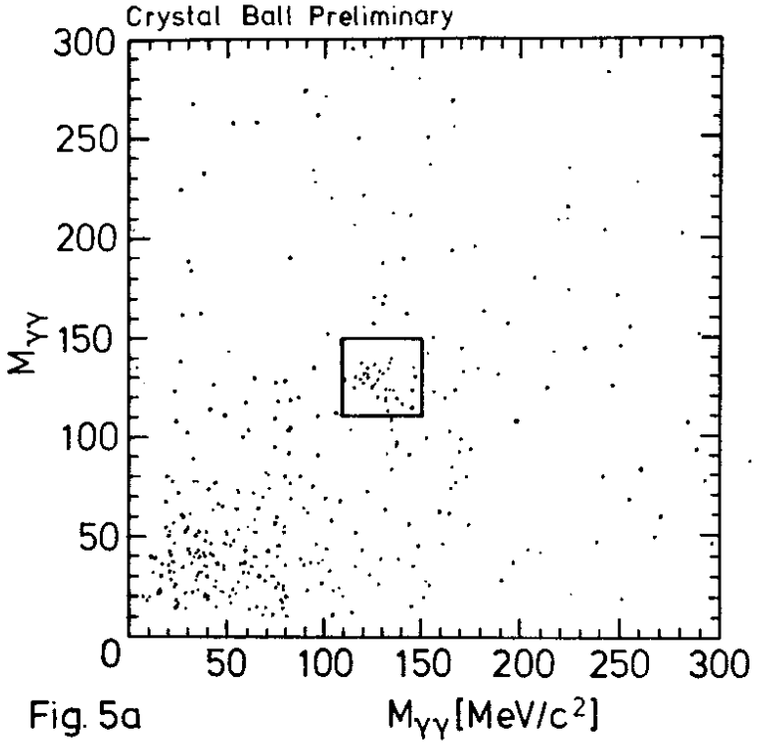
Crystal Ball Preliminary
M_γγ
300
250
200
150
100
50
0
50 100 150 200 250 300
M_γγ [MeV/c²]

Fig. 5a

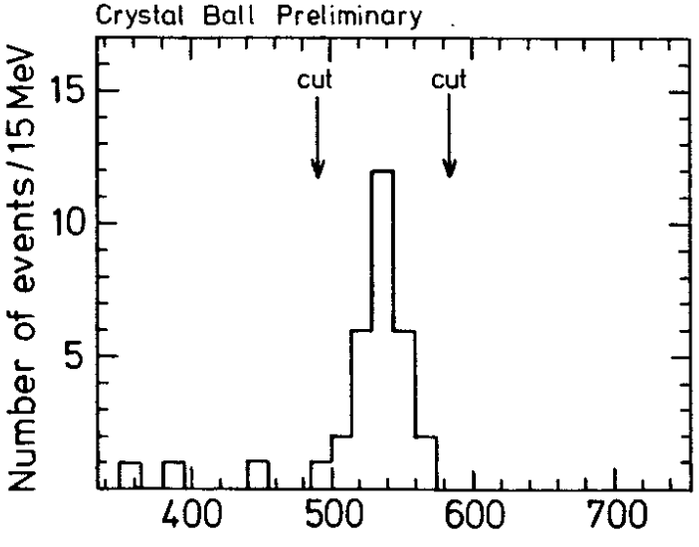
Crystal Ball Preliminary
cut
cut
Number of events/15 MeV
15
10
5
400 500 600 700
M(Υ(2S))-M_Recoil [MeV/c²]

Fig. 5b

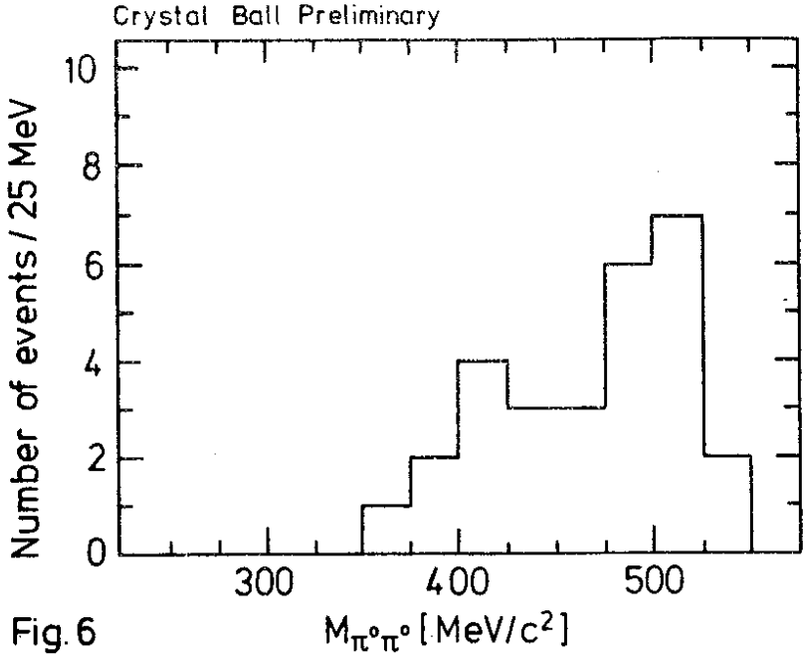
Crystal Ball Preliminary
Number of events / 25 MeV
0
2
4
6
8
10
300
400
500
$M_{\pi^0\pi^0}$ [MeV/$c^2$]

Fig. 6

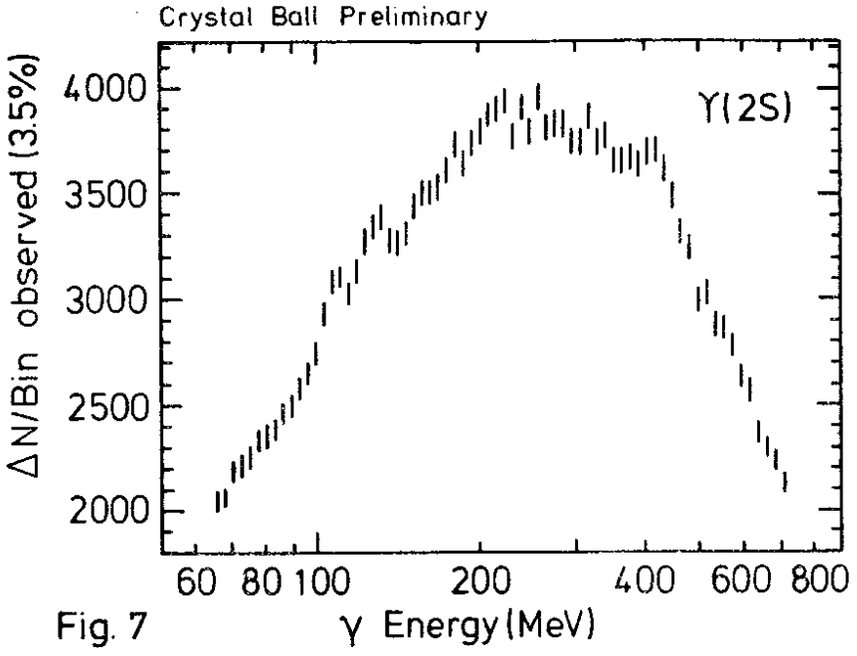
Crystal Ball Preliminary
Υ(2S)
ΔN/Bin observed (3.5%)
2000
2500
3000
3500
4000
60
80
100
200
400
600
800
γ Energy (MeV)

Fig. 7

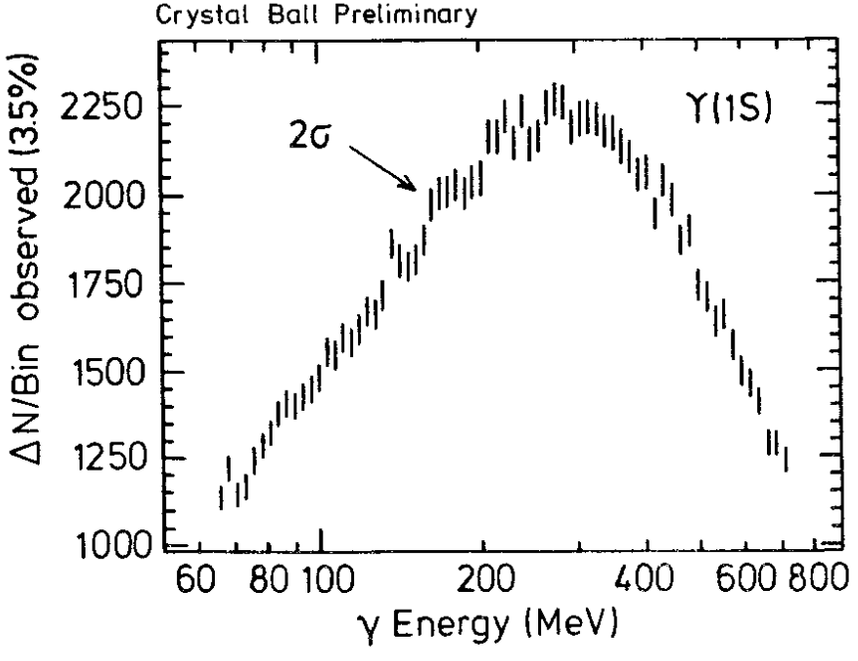
Crystal Ball Preliminary
Υ(1S)
2σ
ΔN/Bin observed (3.5%)
1000
1250
1500
1750
2000
2250
60
80
100
200
400
600
800
γ Energy (MeV)

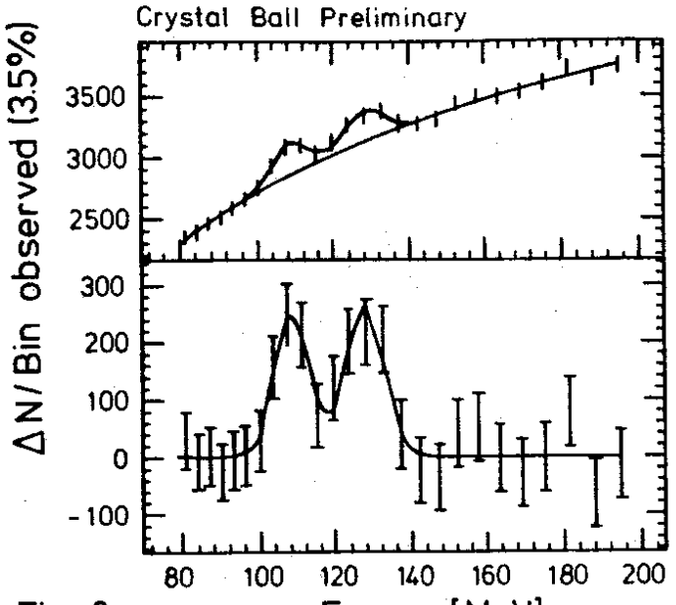


Fig. 8a

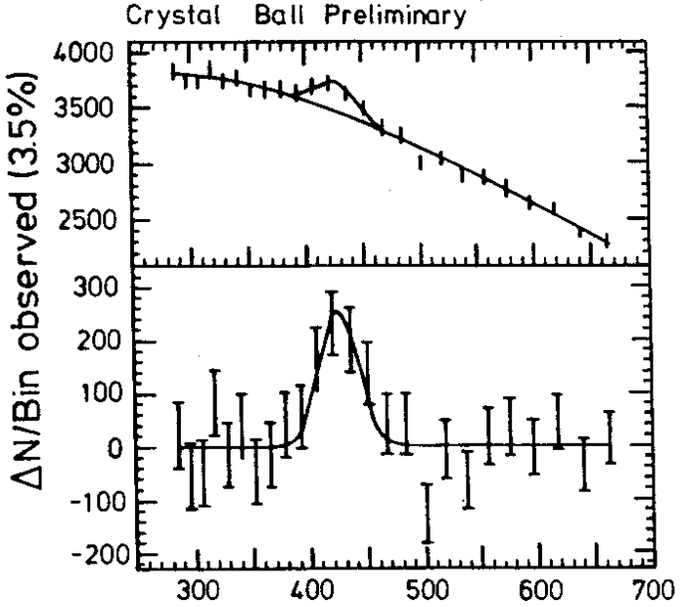


Fig. 8b

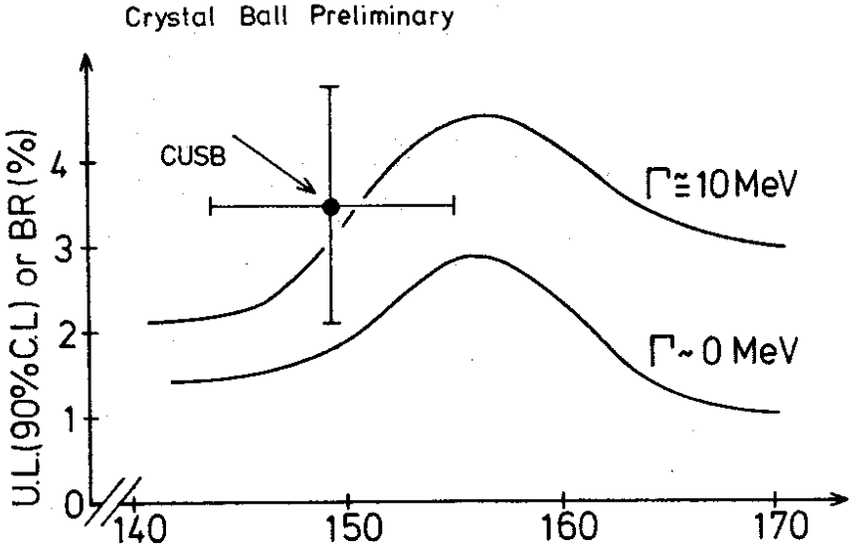


Fig. 9

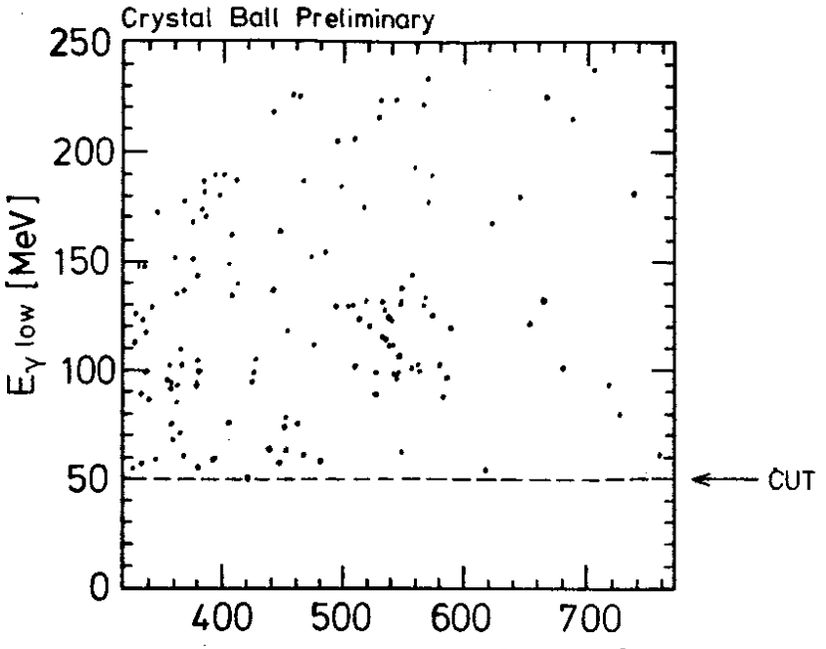


Fig. 10a $M(\Upsilon(2S))-M_{Recoil}[MeV/c^2]$

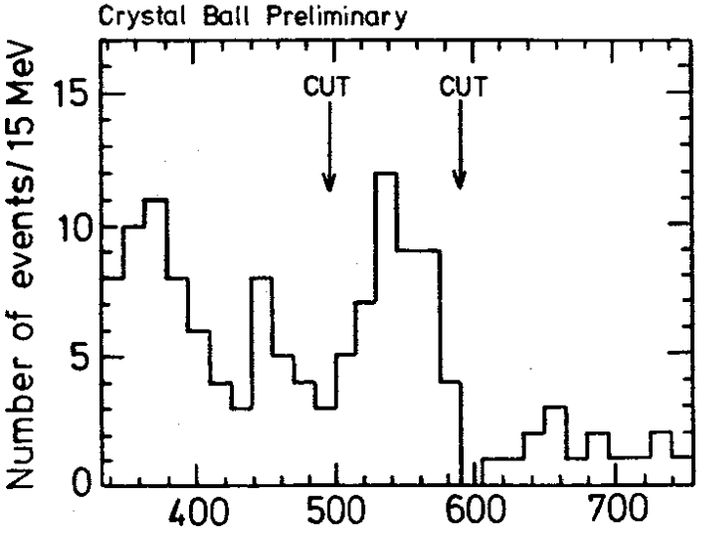


Fig. 10b $M(\Upsilon(2S))-M_{Recoil}[MeV/c^2]$

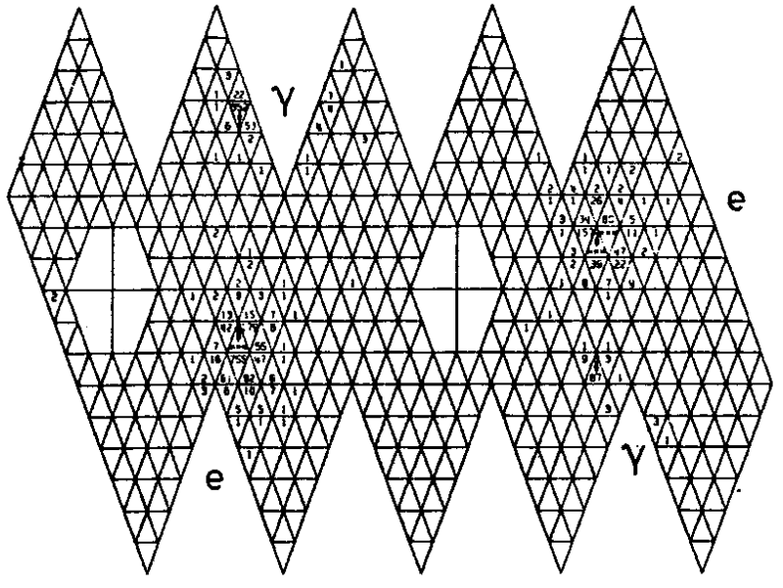


Fig. 11a

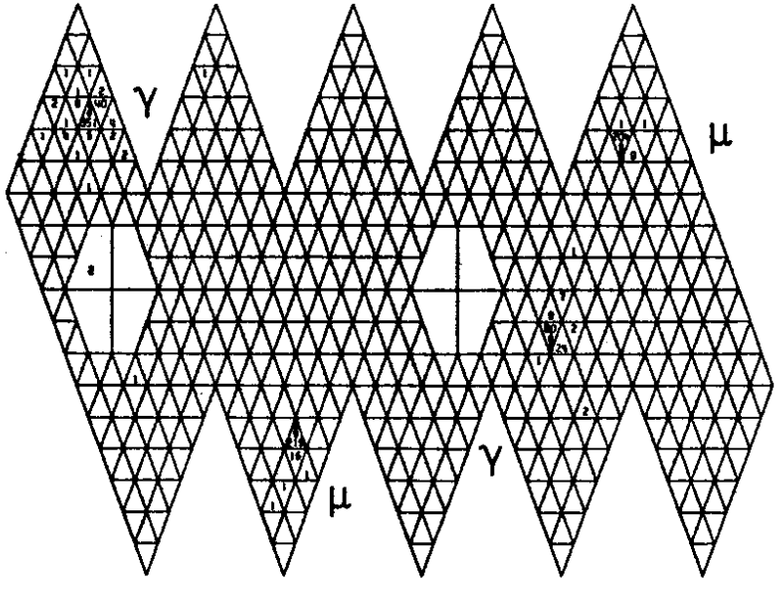


Fig. 11b

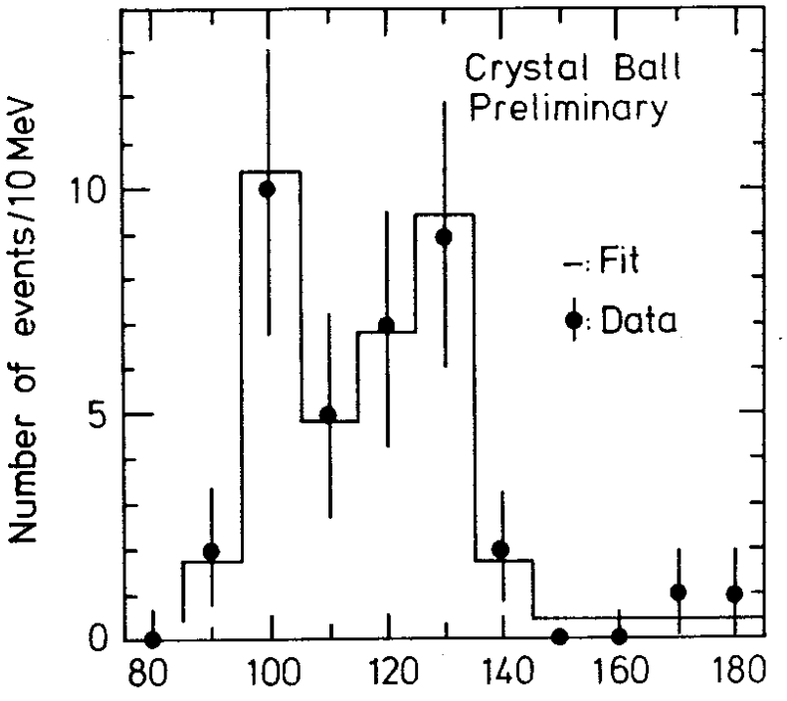
Crystal Ball
Preliminary
—: Fit
●: Data
Number of events/10 MeV
0
5
10
80
100
120
140
160
180
$E_\gamma$(low)[MeV]

Fig. 12